

Component Design

Mini Trash Compactor

AMNSSS Engineering

Alvin Reji

Marlena Eichelroth

Nathaniel Boutin

Salim Hamzaoui

Sandra Chai

Suyash Gundecha

ME 4550 – Mechanical Engineering Design

Prof. Yusti Tjiptowidjojo

Table of Contents

Table of Contents.....	1
Project Summary:.....	3
Design Specifications.....	4
Definitions and Symbols.....	5
Drawings, Illustrations and Models.....	6
Static Failure Analysis.....	7
Buckling Failure Analysis.....	10
Fatigue Failure Analysis.....	11
Appendices.....	13
Appendix A: Team Contribution.....	13
Appendix B: Static Failure Analysis Detailed Explanation.....	14
Appendix C: Buckling Failure Analysis Detailed Explanation.....	18
Appendix D: Fatigue Failure Analysis Detailed Explanation.....	21

Project Summary:

Municipal solid waste management (MSWM) is an increasingly important issue with growing populations and changes in lifestyles leading to much greater amounts of waste produced per capita. Appropriate waste management has far-reaching impacts, spanning from effects on public health, economies, and climate change. Shortages of landfill space, difficulties in collecting large volumes of trash in developing areas, and greenhouse gas emissions from more frequent waste transportation are all motivations for devising a more accessible method of reducing the volume of solid waste through creation of household trash compactors. Many trash compact compactors are either too large, expansive, or high in energy consumption for household use. As a result, there is a need for a more compact, affordable and manageable device, which can be integrated into small spaces. This small compactor can serve small apartments, dorms, or offices where full sized solutions are not feasible.

After further exploration, our team developed the Mini Trash Compactor, a motorized device designed to compact household waste while being easily affordable and efficient. The device utilizes an electric motor connected to a belt system, driving dual lead screws. These screws control the vertical motion of the ram, creating a crushing force when moving down the frame to the bottom of the waste bin, ultimately crushing any items in the process. Once the compaction process is complete, the user can open the drawer and remove the bin to access the compacted items. This mechanism ensures effective and consistent compaction without relying on bulky hydraulic or pneumatic systems typically found in the preexisting models.

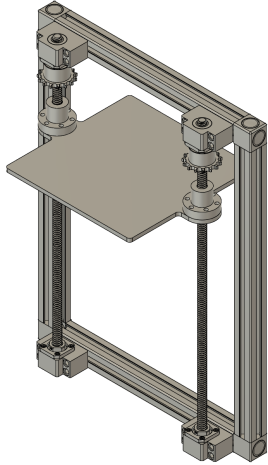


Figure 1 - CAD model of our trash compactor without exterior housing and belt motor system

Design Specifications

Combating the pre existing models, our product must meet design specifications in order to be useful for the consumers. Thus, each design component has their own specifications and the product itself has an overall criteria to meet. The overall device specifications include:

- Dimensions approximately 14" W X 16" D X 20" H
- Total weight of the product should be about up to 25 lb to ensure portability
- Power to be standard 120 AC input from wall socket
- Should last 1000 cycles per year for 5 years, totaling 5000 cycles
- Components must withstand loads required to crush a full bin of aluminum cans and paper
- Ram is constructed of ANSI 330 Stainless Steel
- Lead screws constructed of AISI 1018 Steel

In order to actually build the product, the most important component to meet specifications would be the frame. The frame specifications contains:

- Should be able to withstand a vertical load of 200N applied to the top of the frame
- Protect the mechanism from external forces and possible wear and tear/damage

- Object should remain stationary during cycle
- Never change the orientation of the product
- Constructed of 6061 Aluminum

Definitions and Symbols

L, w, x, h, t, d, r – Frame, Screw, and Ram Dimensions

A – Cross-sectional Area

E – Young's Modulus

I – Second Moment of Inertia

F – Applied Forces

M – Moment

R – Reaction Forces

n – Factor of Safety

n_y – Yielding Safety Factor

$n_{fatigue}$ – Fatigue Safety Factor

$\sigma_{a0}, \sigma_m, \sigma_a$ – Stress (nominal, mean, amplitude)

S_y – Yield Strength

S_r – Slenderness Ratio

P_{cr} – Critical Load

C_c – Critical Slenderness Ratio

k – Radius of Gyration

C – End Condition Constant

S_{ut} – Ultimate Tensile Strength

S_{ut}' – Ultimate Tensile Strength Considering Temperature

S_e – Endurance Limit

S'_e – Modified Endurance Limit

k_a, k_b, k_c, k_d, k_e – Factors (surface, size, loading, temperature, reliability)

Drawings, Illustrations and Models

Included below are models of our device with component and dimension call outs. The compactor consists of a t-slot frame connected by t-slot brackets. The lead screws connect to the top and bottom frame members via end supports that have t-slot nuts. A flange nut attaches each side of the ram to the lead screw. On each set screw between the flange nut and the upper end support is a sprocket that will hold the belt that is driven by a motor to rotate the screws and move the ram vertically.

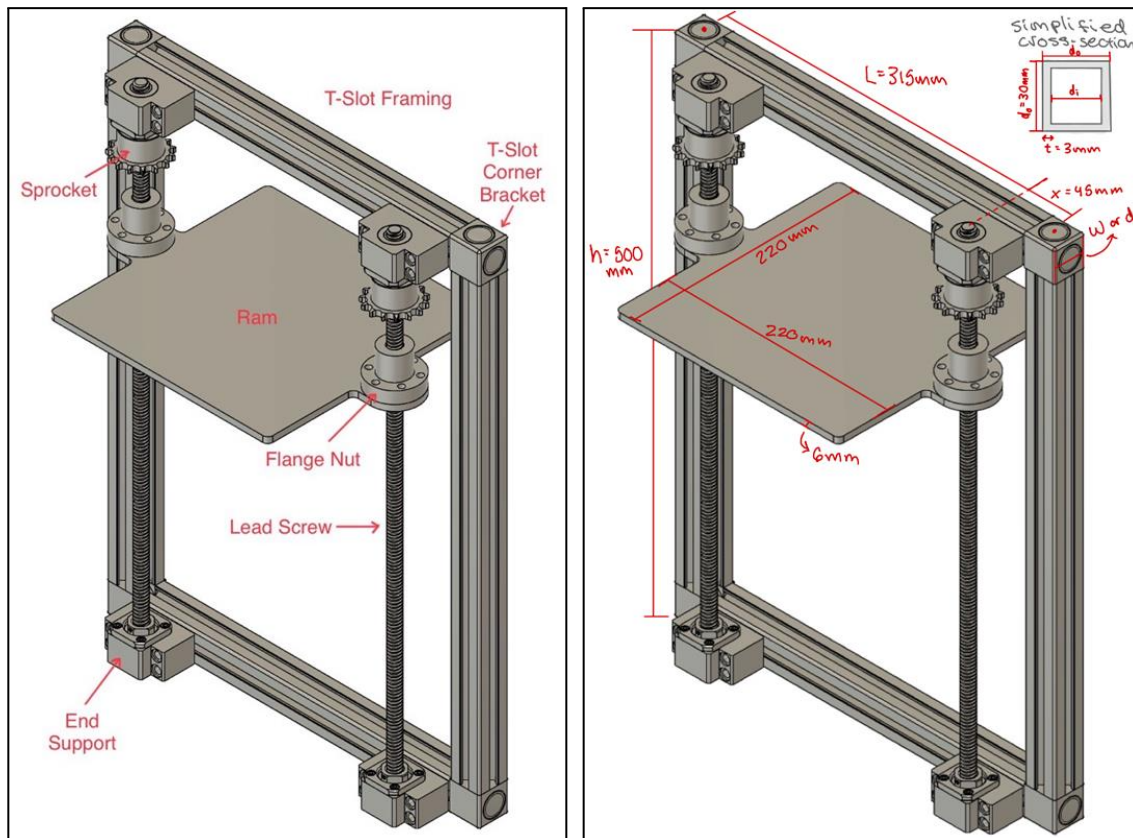


Figure 2 - Assembly with component call outs and assembly with dimensions

After much discussion we agreed that the frame, lead screws, and ram were the main components we needed to analyze for the component design portion of the project. The horizontal and vertical beams of the frame are exposed to static failure due to the forces it experiences from the lead screws and ram as an object is being compressed. The lead screws are exposed to buckling failure based on the reaction forces experienced from crushing an object. The crushing force experienced by the entire compactor is introduced at the ram, therefore we decided to analyse fatiguing on the ram.

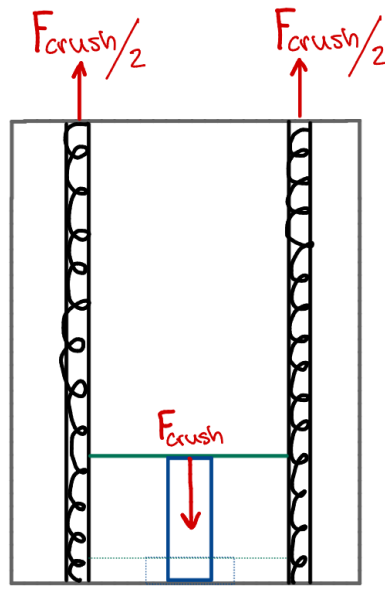


Figure 3 - Static failure loading condition

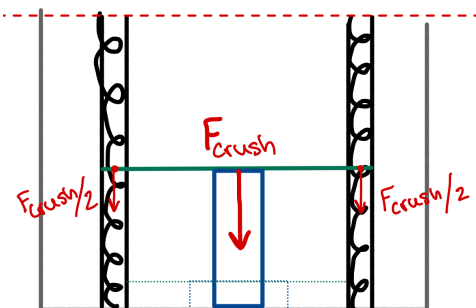


Figure 4 - Buckling failure loading condition

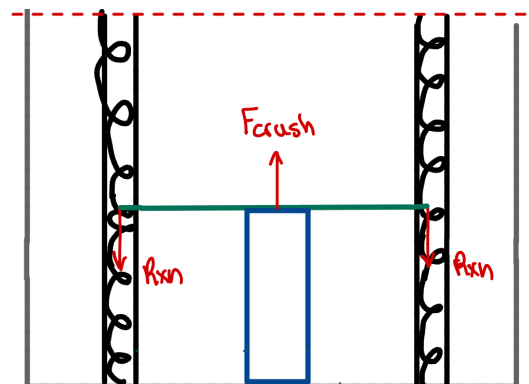


Figure 5 - Fatigue failure loading condition

Material Properties

Steel AISI 1018	330 Stainless Steel	6061 Aluminum
$S_y = 572 \text{ MPa}$ $S_{ut}' = 696 \text{ MPa}$ $E = 207 \text{ GPa}$	$S_y = 276 \text{ MPa}$ $S_{ut}' = 568 \text{ MPa}$ $E = 200 \text{ GPA}$	$S_y = 275 \text{ MPa}$ $S_{ut}' = 310 \text{ MPa}$ $E = 68.9 \text{ GPa}$

Static Failure Analysis

The static loading configuration with the highest probability of failure on the frame would occur at the top most member of the frame with two upward forces acting upon the frame from the lead screws. The two forces on the top beam are influenced by the force it takes to crush an object under the ram that is driven by the two lead screws. The maximum crushing force our device is designed to handle is 200N, and we assumed this force is evenly distributed between the two lead screws, therefore two 100N loads on the top beam is the worst case scenario we will examine in this analysis. We will also look at how these loads affect the left and right vertical beams of the frame.

The corners of the frame were treated as simple supports. Two 100N point loads, F , are applied on the top beam of length L at distance x from each end of the beam. When defining the moment of inertia to find the stress, we simplified the geometry of the beam to a hollow square of width w and wall thickness t . The von Misses stress is calculated as follows:

$$(\sigma_0)_{bending} = \frac{M_{maximum} * r}{I}, \quad (\text{Equ. 1})$$

$$\text{where } I = \frac{d_{outer}^4 - d_{inner}^4}{12} \quad (\text{Equ. 2})$$

$$\therefore \sigma_0 = 16.94 \text{ MPa}$$

The safety factor for the top beam was calculated using yield strength for 6061 Aluminum obtained from the Fusion360 native library.

$$n = \frac{S_y}{\sigma_0} = 16.23 \quad (\text{Equ.3})$$

Static failure of the top beam was demonstrated using FEA in Fusion360. The maximum bending stress according to the simulation is 13.687 MPa and occurs at the left and right most points of the beam and on the front side where the lead screws are attached via the beam's t-slots and end supports. The 3.253 MPa discrepancy can be attributed to our simplification of the beam's geometry from t-slot to a hollow square extrusion for the second moment of inertia.

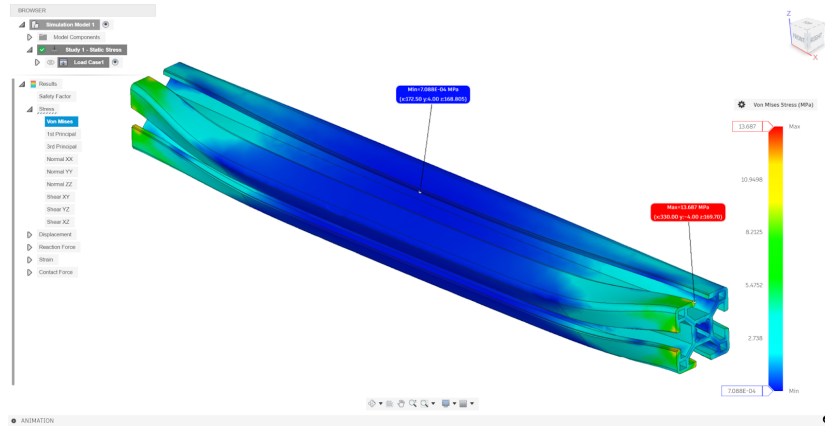


Figure 6 - FEA of frame's top beam

The two supporting beams on the left and right sides of the frame also experience some static loading due to the reaction forces from the top and bottom beam. These reaction forces are also as a result of the crushing forces applied to lead screws from the ram. This creates an axial stress calculated from a force of 100 N on both beams as it acts perpendicular to the beam's central axis.

$$(\sigma_0)_{Axial} = \frac{F}{A} \quad (\text{Equ. 4})$$

$$\text{Where } A = \frac{\pi}{4} (D)^2 \quad (\text{Equ. 5})$$

With an outside diameter of 30mm and thickness of 3mm, our value for D to calculate the area is 6mm. This gives us an axial stress of 3.537 for one of the side beams. Using equation 3 above and a yield strength S_y of 275 MPa for the 6061 Aluminium, the safety factor of 77.75 was found, indicating this aluminium is more than capable of supporting the loads the vertical beams experience. The maximum stress according to the FEA is 0.3672 MPa.

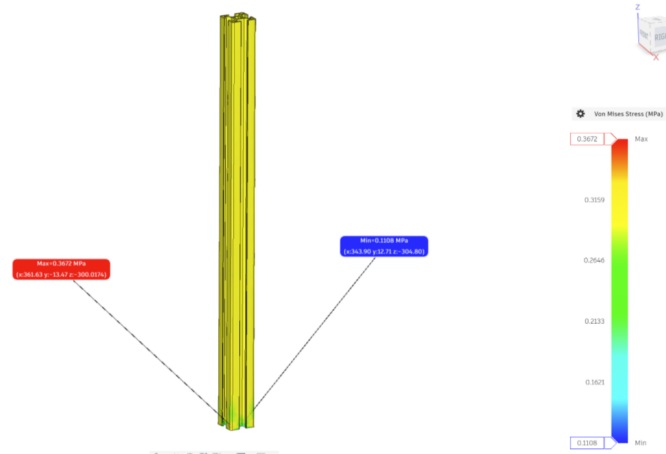
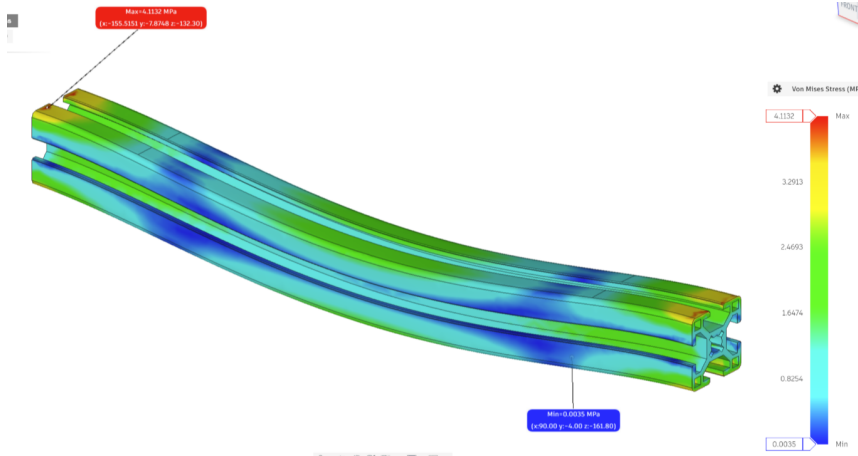


Figure 7 - FEA of the vertical beams

The bottom beam of the frame sees both bending and direct shear. Analysis was performed on the bottom beam of the structure which sees a distributed force exerted by the trash bin, and two counteracting moments at either end of the beam from the vertical T-slot framing supports. The distributed load from the trash bin generates compressive bending on the beam while the two counteracting moments from the vertical support generate a counteracting tension to keep the beam in equilibrium. On the front face of the beam, the brackets exert a force in the positive z-direction while the bracket screws exert a force in the negative z-direction. Since the brackets and screws exert equal and opposite forces at the same location, direct shear is generated.



Buckling Failure Analysis

The most likely element to experience buckling failure would be due to a vertical force acting at the lead screw connection point between the ram and the frame. This force would be applied during the actual compaction of tin cans when the product is in use. Here we will treat the ends of the lead screws as rounded, so the recommended C value used is $C = 1$.

$$C_c = \sqrt{\frac{2C\pi^2 E}{S_y}} = \sqrt{\frac{2*1*\pi^2*207000}{572}} = 84.518 \text{ (Equ.5)}$$

$$S_{R-Midway} = \frac{L}{k} = \frac{235 \text{ mm}}{2.25 \text{ mm}} = 104.4 \text{ (Equ.6)}$$

$$S_{R-Full} = \frac{L}{k} = \frac{470 \text{ mm}}{2.25 \text{ mm}} = 208.8 \text{ (Equ.7)}$$

The critical slenderness ratio value found was to be 84.518, while both slenderness ratios were found to be larger than the critical slenderness ratio ($S_R >> C_c$). Therefore we can use the Euler Buckling Equation to govern how the lead screw behaves under applied force.

$$P_{CR-Midway} = \frac{C\pi^2 EI}{L^2} = 11.9 \text{ kN} \text{ (Equ.8)}$$

$$P_{CR-Full} = \frac{C\pi^2 EI}{L^2} = 2.98 \text{ kN} \text{ (Equ.9)}$$

$$n = \frac{P_{CR}}{A_y} = 29.8 \text{ (Eqn.10)}$$

Thus the lowest critical load, P_{CR} , is 2.98 kN, and the factor of safety is 29.8. This was further verified by conducting an FEA analysis of the screw, resulting in the factor of safety value of 30.36, close to the value found by our hand calculations. Overall, since our factor of safety is above 1, the screws resist buckling.

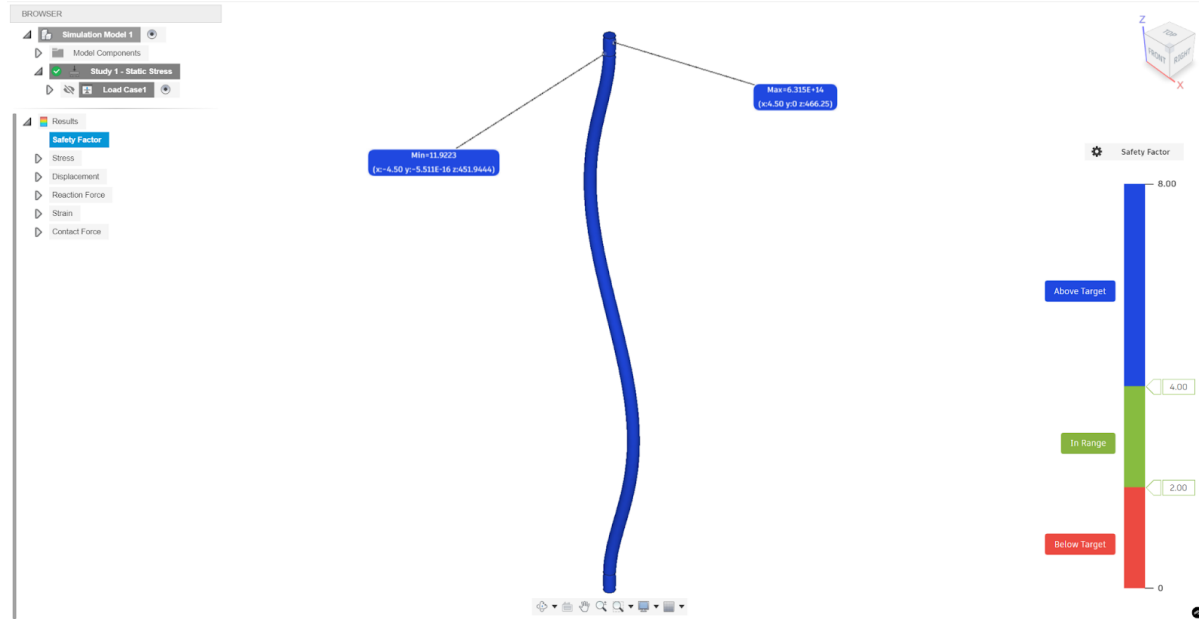


Figure 8 - FEA Analysis for Lead Screws

Fatigue Failure Analysis

The ram is subject to fatigue failure since it faces cyclic loads. Cycles of varying stress are found when a maximum stress is applied while the ram is compacting the cans, and a lack of stress when the ram is not operational. The distributed load from the trash pushing upon the ram results in bending of the ram. A bending analysis was first conducted to find the maximum moment applied on the component and resulted in a value of 4.17 MPa. Information on how this value was found can be found in Appendix D.

However, this value wasn't as accurate because we simplified the geometry of our ram to a square beam. The addition of the circular flanges that attach to flange nuts greatly influences the results. After

running an FEA simulation, a more accurate value of 15.1 MPa was calculated, which will be the value used for fatigue analysis later on.

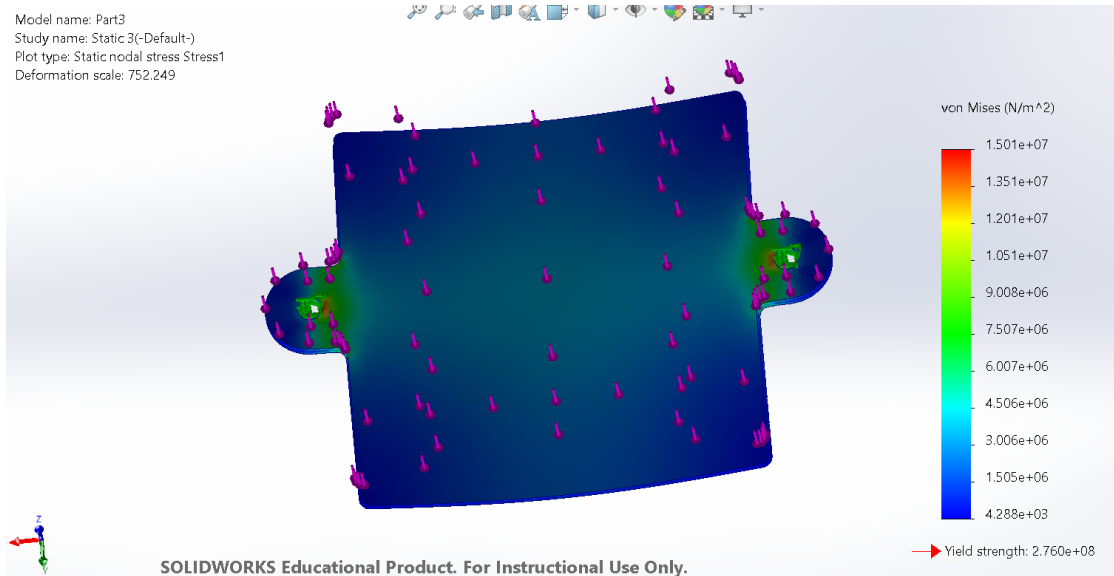


Figure 9: FEA Analysis for Ram

Since the maximum and minimum values of stress applied were known to be 15 MPa and 0 MPa respectively, we found the stress amplitude and mean using the equations below:

$$\sigma_a = \frac{\sigma_{max} - \sigma_{min}}{2} = 7.5 \text{ MPa} \text{ (Equ. 11)}$$

$$\sigma_m = \frac{\sigma_{max} + \sigma_{min}}{2} = 7.5 \text{ MPa} \text{ (Equ. 12)}$$

The endurance strength/limit was found by taking into account material, size, and loading factors and resulted in $S_e = 143.86 \text{ MPa}$. The exact calculations for this value are found in Appendix D. Since our maximum stress was well below the endurance strength, we were in the infinite life domain of the stress-cycle curve. The factor of safety for the fatigue was found to be 15.31.

$$n_{fatigue} = \left(\frac{\sigma_a}{S_e} + \frac{\sigma_m}{S_{ut}} \right)^{-1} = \left(\frac{7.5}{143.86} + \frac{7.5}{568} \right)^{-1} = 15.31 \text{ (Equ. 13)}$$

Since the safety factor is greater than 1, this again verifies that the ram is expected to have infinite life. The localized yielding was also found in a similar manner and resulted in a yielding safety factor of 18.4.

$$n_y = \frac{S_y}{\sigma_m + \sigma_a} = \frac{276}{7.5 + 7.5} = 18.4 \text{ (Equ. 14)}$$

Since this factor of safety is above 1, the ram will not yield during its cyclic use.

Appendices

Appendix A: Team Contribution

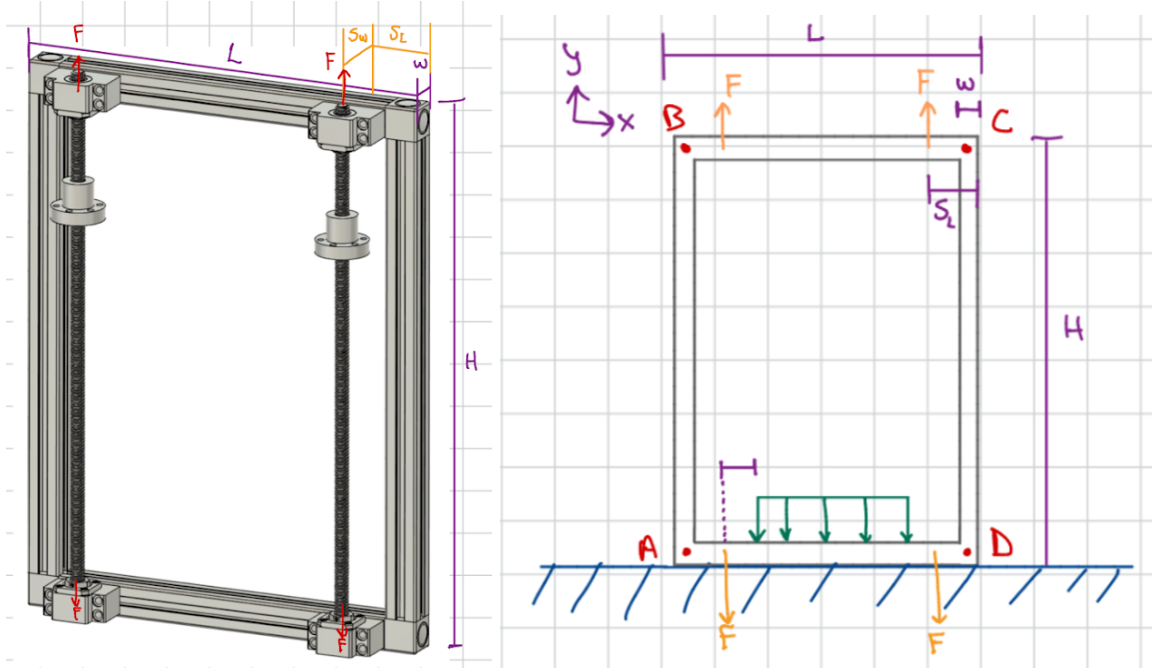
Below is a table with the individual contributions of team members to the Components Design Report.

The team met several times to discuss relevant loads and solving strategies. All members contributed to report writing.

Member	Responsibilities
Alvin Reji	Initial FBD of Buckling Failure Analysis; Initial FBD of Fatigue Failure Analysis, Fatigue Failure Report
Marlena Eichelroth	Initial FBD and force analyses of frame; static failure analysis report section; drawing, illustrations, and models section; editing for cohesion
Nathaniel Boutin	FEA Analysis of Static Failure, Buckling Failure, Fatigue Failure Analysis; CAD modelling;
Salim Hamzaoui	Initial FBD of Static Failure Analysis;
Sandra Chai	Initial FBD of Buckling Failure Analysis; CAD modelling, report writing for bottom beam
Suyash Gundecha	Static failure analysis report section calculations and appendix; Project Summary;

Appendix B: Static Failure Analysis Detailed Explanation

The static loading configuration with the highest chance of failure would be the top horizontal bar of the frame with the lead screws connecting to it.



Figures 10 and 11 - Free-Body Diagram of frame

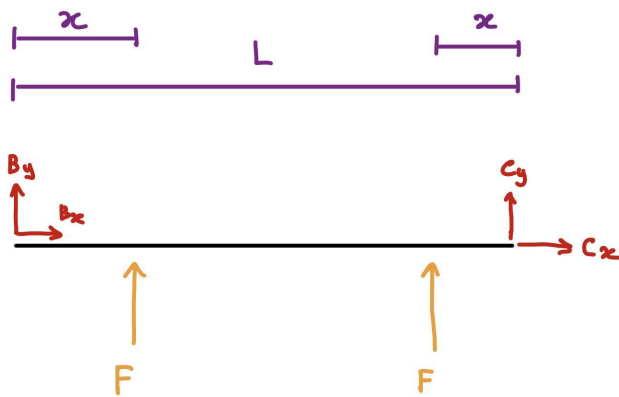


Figure 12 - Free-Body Diagram of Top Frame Member BC

$$\Sigma F_y = B_y + C_y + 2F = 0$$

$$\Sigma M_B = LC_y + (L - x)F + xF = 0$$

$$C_y = -F$$

$$B_y = -F$$

F was found to be 100 N since the average force required to crush can be 200 N. The force is split between the two lead screws, equating to be 100 N of force through each screw. The length L is 345 mm.

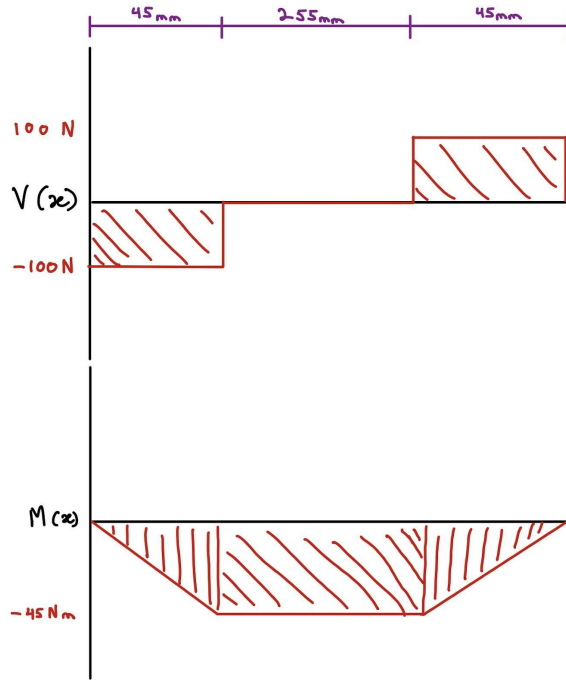


Figure 13 - Shear Force and Moment Diagram for Member BC

$$V_1 = -100 \text{ N}$$

$$V_2 = 0 \text{ N}$$

$$V_3 = 100 \text{ N}$$

$$M_1 = -100x \text{ Nm}$$

$$M_2 = -45 \text{ Nm}$$

$$M_3 = 100x - 45 \text{ Nm}$$

Thus, maximum bending moment appears at the section in between both lead screws, amounting to 45 N-m. The nominal bending stress at this location can be calculated by:

$$(\sigma_0)_{bending} = \frac{M_{maximum} * r}{I}$$

Where r is the radius of the beam, I is the moment of inertia. The moment of inertia can be calculated by the following:

$$I = \frac{d_{outer}^4 - d_{inner}^4}{12}$$

Where the outer diameter is 30 mm, the inner diameter is 24 mm. Thus resulting in the moment of inertia I being 39852 mm^4 . Thus, the bending stress equates σ_0 to 16.94 MPa.

Using the bending stress and the yield strength for 6061 Aluminium, the safety factor against static failure of the top beam is:

$$n = \frac{s_y}{\sigma_0} = \frac{275}{16.94} = 16.23$$

The other components of the compactor experiencing static loading are left and right beams of the frame which are attached to the top and bottom beams such as member BC as shown in figure 11.



Figure 14 - Free-Body Diagram of Left Frame Member AB

Here, the forces of Ay and By are both the same magnitude as F above, which was found to be 100 N. The length L in this case is 440 mm.

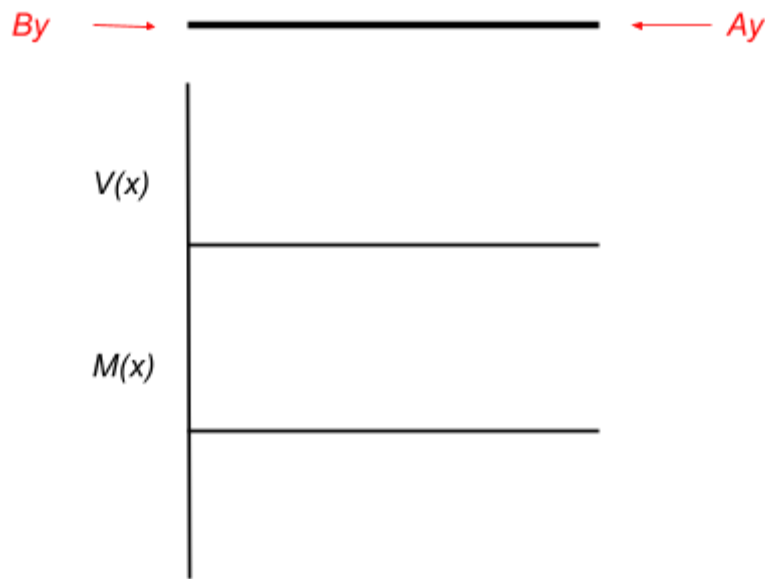


Figure 15 - Shear Force and Moment Diagram for Member AB

As seen from the shear and moment diagrams for the beam, there is no moment as the forces are acting in parallel to the neutral axis. However, the axial stress can be found using the forces from Ay and By:

$$(\sigma_0)_{Axial} = \frac{F}{A}$$

Where F is the force of Ay and By equal to 100 N. Using the diameter of 30mm and thickness of 3mm for the beams, we have a cross sectional area of 28.27mm^4 . This gives us an axial stress of 3.537 MPa.

Using the same methods as the top beam, we can find a factor of safety for the bottom beam of 77.75.

$$n = \frac{s_y}{\sigma_0} = \frac{275}{3.537} = 77.75$$

Analysis of the bottom beam of the frame requires looking at the forces in 3D. A free-body diagram of the bottom beam is shown below:

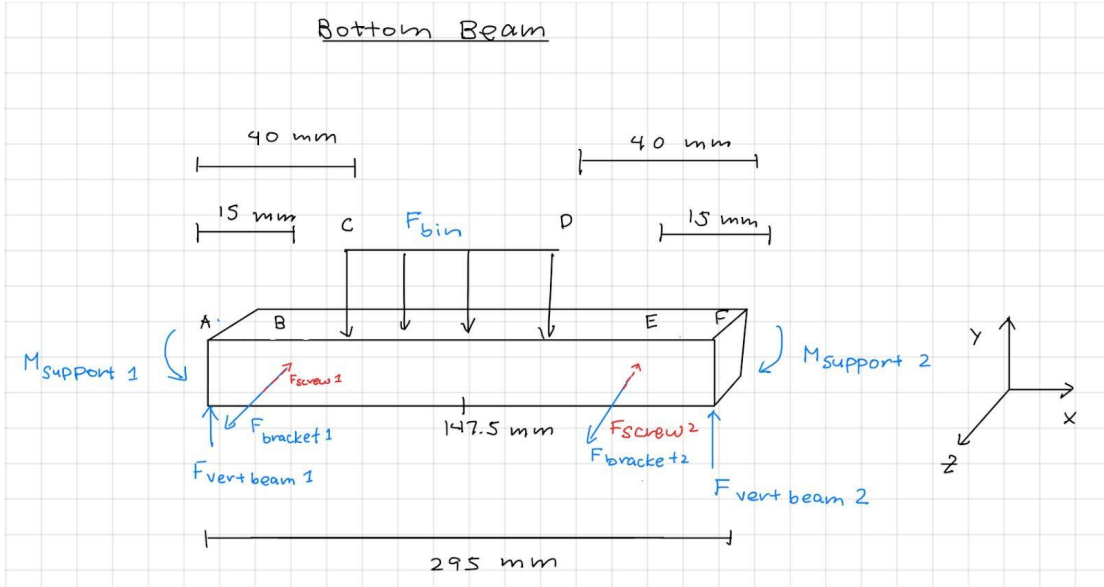


Figure 16 - Free-body diagram of the bottom beam

Summing the forces in the y-direction for the force of the bin, the force of the vertical beams Member AB and Member CD, the following force balance equation was created:

$$\Sigma F_y = -F_{bin}(215mm) + 2F_{verticalbeam} = 0$$

Finding the sum of the moments about point A, the following moment balance was created:

$$\Sigma M_A = M_{support1} - F_{bin}(215mm)(147.5mm) + F_{verticalbeam}(295mm) - M_{support2}$$

Since the structure is symmetrical and the loadings are the same in magnitude but in opposite directions,

$$M_{support1} = M_{support2}$$

In the z-direction, the force of the brackets and screws act at the same point, but in opposite directions.

This generates direct shear at points B and E on Figure 16. The following equation for direct shear was found:

$$\tau = \frac{4V}{3A} = \frac{4F_{screw1}}{3\pi r_{screw}^2}$$

Appendix C: Buckling Failure Analysis Detailed Explanation

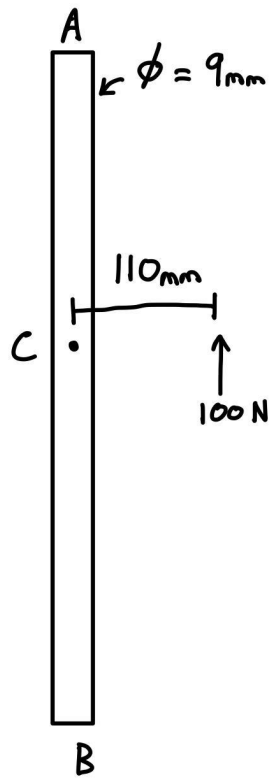


Figure 16 - Lead Screw Moment Calculation

We can find the moment around point C by solving the reactions:

$$M_c = 100 * 0.110 = 11 \text{ Nm}$$

The material used for the lead screws is Steel AISI 1018, the Young's Modulus and Yield Strength was found from the Fusion 360 native libraries archive,

$$E = 207 \text{ GPa}$$

$$S_y = 572 \text{ MPa}$$

Thus,

$$r = d/2 = 4.5 \text{ mm}$$

$$A = \pi r^2 = \pi * 4.5^2 = 63.62 \text{ mm}^2$$

$$I = \frac{\pi}{4} * r^4 = \frac{\pi}{4} * 4.5^4 = 1017.876 = 322.06 \text{ mm}^4$$

$$k = \sqrt{\frac{I}{A}} = 2.25 \text{ mm}$$

As the lead screw is constrained against rounded-rounded end conditions (pin-roller), we can use the recommended C value of 1 for our calculations.

$$C_c = \sqrt{\frac{2C\pi^2E}{S_y}} = \sqrt{\frac{2*1*\pi^2*207000}{572}} = 84.518$$

Thus the slenderness ratio at the midway section can be calculated by:

$$S_{R-Midway} = \frac{L}{k} = \frac{235 \text{ mm}}{2.25 \text{ mm}} = 104.4$$

The midway point was analyzed because it was a point of interest. The more likely element subjected to buckling is the screw considering its entire length. The slenderness ratio for the entire screw can be calculated by:

$$S_{R-Full} = \frac{L}{k} = \frac{470 \text{ mm}}{2.25 \text{ mm}} = 208.8$$

Thus, as our $S_R \gg C_c$, the Euler Buckling method will be used to solve for the factor of safety.

$$P_{CR} = \frac{C\pi^2EI}{L^2}$$

$$P_{CR-Midway} = \frac{C\pi^2EI}{L^2} = \frac{1*\pi^2*207000*322.06}{235^2} = 11914.4 \text{ N} = 11.9 \text{ kN}$$

$$P_{CR-Full} = \frac{C\pi^2EI}{L^2} = \frac{1*\pi^2*207000*322.06}{470^2} = 2978.6 \text{ N} = 2.98 \text{ kN}$$

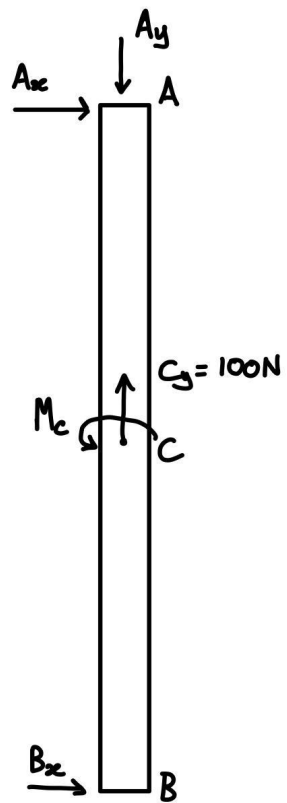


Figure 17 - Lead Screw Reaction Force Calculation

$$\Sigma F_y = C_y - A_y = 0$$

$$A_y = C_y = 100 \text{ N}$$

Thus, using the lowest P_{CR} value being 2.98 kN and the reaction force at A_y , we can calculate the factor of

safety for buckling by using the following formula:

$$n = \frac{P_{CR}}{A_y} = \frac{2.98 \text{ kN}}{100 \text{ N}} = 29.8$$

Appendix D: Fatigue Failure Analysis Detailed Explanation

Figure 18 below showcases the free body diagram of the ram along with the shear and moment diagrams.

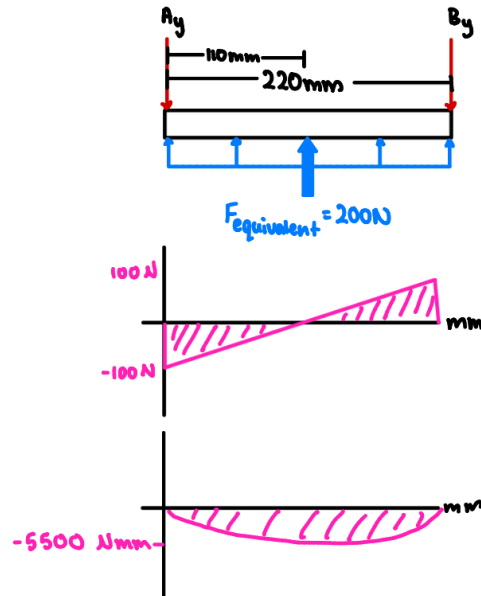


Figure 18 - FBD, Shear, and Moment Diagrams of the ram

$$\Sigma F_y = F_E - A_y - B_y = 0$$

Due to the symmetry of the problem, \$A_y = B_y\$, thus:

$$\Sigma F_y = F_E - A_y - A_y = 0$$

$$F_E = 2A_y$$

$$A_y = B_y = 100N$$

Equations for the shear and moment diagrams were calculated and seen below

$$V(x) = \frac{200}{220}x - 100$$

$$M(x) = \frac{100}{220}x - 100x$$

The maximum moment was located at the center of the ram or when \$x = 110 \text{ m}\$. At this location, the moment was found to be \$-5500 \text{ Nmm}\$ or \$-5.5 \text{ Nm}\$. The moment of inertia for the ram was simplified to a square beam which can be defined as seen below.

$$I = \frac{bh^3}{12} = \frac{(220)(6)^3}{12} = 3960mm^4$$

This value would be used alongside the maximum moment to find the bending stress within the beam.

Calculating this value resulted in a maximum bending stress of 4.17 MPa.

$$\sigma = \frac{Mc}{I} = \frac{(5500)(6/2)}{3960} = 4.17 MPa$$

However this oversimplification of our inertia skews our results, leading us to use the data from our FEA simulation. The ram would be subject to a cyclic load where it would reach a maximum stress of 15 MPa (from our FEA results) and a minimum stress of 0 MPa. This section aims to explain if fatigue would present itself as an area of concern, as one of our main considerations was that this mechanism should be able to run a thousand cycles per year for a total of 5 years. Figure 19 below demonstrates the Zero to Tensioning Cyclic Stress that our mechanism would have to endure.

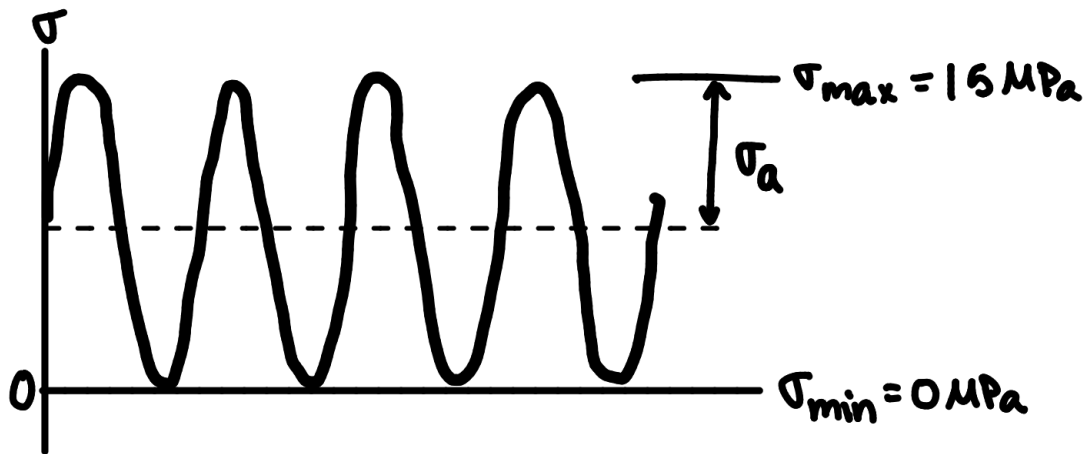


Figure 19 - Zero to Tensioning

The ram would experience maximum stress during its compaction and no stress while it rests without operating. The mean stress and stress amplitude were found to be

$$\sigma_a = \frac{\sigma_{max} - \sigma_{min}}{2} = 7.5. MPa$$

$$\sigma_m = \frac{\sigma_{max} + \sigma_{min}}{2} = 7.5 MPa$$

Using Table-A22, the yield strength and ultimate tensile strength for 304 SS (stainless steel) was found to be

$$S_y = 276 \text{ MPa}$$

$$S_{ut}' = 568 \text{ MPa}$$

The assumption of operating at room temperature gave a correction factor $k_d = 1$. The temperature dependent maximum tensile strength (S_{ut}) was then determined to be

$$S_{ut} = k_d * S_{ut}' = 1 * 568 = 568 \text{ MPa}$$

For a Cold-Drawn Finish, the values for a and b were using Table 6-2,

$$a = 3.04$$

$$b = -0.217$$

Plugging these values into Equation 6-18 resulted in a surface factor k_a as seen below.

$$k_a = a * S_{ut}^b = 3.04 * (568)^{-0.217} = 0.768$$

Since the equivalent force proves a bending moment, it would result in a size factor. Due to the rectangular geometry of the ram, the effective diameter of the beam must be found first using Equation 6-24 and by inputting the cross-sectional area of the ram.

$$d_e = 0.808 * \sqrt{bh} = 0.808 * \sqrt{220 * 6} = 29.356 \text{ mm}$$

Using Equation 6-23 for d results in a value of

$$d = \frac{d_e}{0.37} = \frac{29.356}{0.37} = 79.34 \text{ mm}$$

Using the piece-wise function for k_b as seen in Equation 6-19, the size factor was found to be

$$k_b = 1.51 * d^{-0.157} = 1.51(79.34)^{-0.157} = 0.76$$

As the forces acting on the geometry result in bending, the loading factor k_c was determined to be 1. For 95% reliability, Shigley's Table 6-4 gives a reliability factor, $k_e = 0.868$. The endurance limit for the fatigue was determined by halving the ultimate tensile strength as seen below.

$$S_e' = 0.5 * S_{ut}' = 0.5 * 568 = 284 \text{ MPa}$$

By incorporating all of these factors, we can calculate the endurance strength by the following:

$$S_e = k_a k_b k_c k_d k_e S_e'$$

$$S_e = 0.768 * 0.76 * 1 * 1 * 0.868 * 284 = 143.86 \text{ MPa}$$

From this we can understand that our maximum stress is well below the endurance limit of the ram.

Therefore we are well within the infinite life region of the S-N curve seen below.

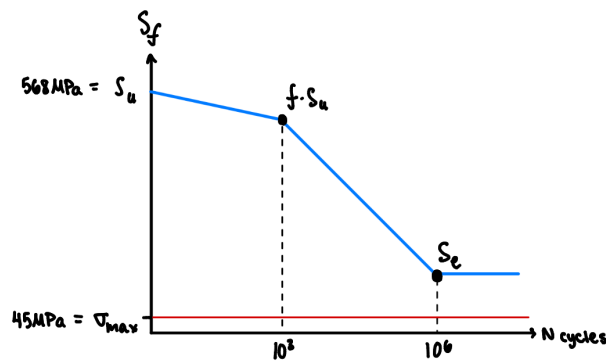


Figure 20 - Stress-Cycle Curve

Finally, we can calculate the safety factor for fatigue since $\sigma_m > 0$.

$$n_{fatigue} = \left(\frac{\sigma_a}{S_e} + \frac{\sigma_m}{S_{ut}} \right)^{-1} = \left(\frac{7.5}{143.86} + \frac{7.5}{568} \right)^{-1} = 15.31$$

Localized yielding can also be checked by finding the yielding safety factor as seen below.

$$n_y = \frac{S_y}{\sigma_m + \sigma_a} = \frac{276}{7.5 + 7.5} = 18.4$$